2010 IEEE International Conference on Robotics and Automation
Anchorage Convention District
May 3-8, 2010, Anchorage, Alaska, USA

3-D Shape Measurement of Pipe by Range Finder Constructed with Omni-Directional Laser and Omni-Directional Camera

Kenki Matsui, Atsushi Yamashita and Toru Kaneko

Abstract— **A lot of plumbings such as gas pipes and water pipes exist in public utilities, factories, power plants and so on. It is difficult for humans to inspect them directly because they are long and narrow. Therefore, automated inspection by robots equipped with camera is desirable, and great efforts have been done to solve this problem. However, many of existing inspection robots have to rotate the camera to record images in piping because a conventional camera with a narrow view can see only one direction while piping has a cylindrical geometry. The use of an omni-directional camera that can take images of 360° in surroundings at a time is effective for the solution of the problem. However, the shape measurement is difficult only with the omni-directional camera. Then, in this paper, we propose a reconstruction method of piping shape by using an omni-directional camera and an omni-directional laser with a light section method and a structure from motion analysis. The validity of the proposed method is shown through experiments.**

I. Introduction

A lot of plumbings such as gas pipes and water pipes exist in public utilities, factories, power plants and so on. These facilities are important and indispensable for our lives.

However, these pipes become deteriorated by aging and internal damage comes to existence. If the damage grows large, a serious accident may happen.

To find such damage at the early stage, and to take precautions against possible accidents, it is important to recognize the pipe state. However it is difficult for humans to inspect the pipe state directly because they are long and narrow and often laid underground. Therefore, automated inspection by robots equipped with camera is desirable and many efforts have been done to solve the problem [1][2][3][4][5][6].

However, many of existing inspection robots have to rotate the camera to record images in piping because a conventional camera with a narrow view can see only one direction while piping has a cylindrical geometry. There is a problem that inspection robot have to stop every time at the point where the robot records the image. Therefore, it takes long time to measure pipe shape.

On the other hand, vision sensors with a wide field of view have been invented; e.g. a fisheye camera and an omni-directional camera. They have a variety of potential applications, such as mobile robot navigation [7], and telepresense technology [8]. Particularly, previous studies showed that an omni-directional camera is effective in measurement and recognition of environment [9].

Kannala et al. proposed a pipe inspection method using omni-directional vision sensor for robot vision [10]. The use of the omni-directional vision sensor that can take images of 360°in surrounding at a time is effective for pipe inspection. They use the structure from motion analysis which is a kind of passive measurement. However, the method has to extract and track feature points to get corresponding points between images. If corresponding point detection fails, the measurement accuracy decreases.

To solve this problem, a light section method which is a kind of active measurement is proposed instead of passive measurement like the structure from motion. The light section method has an advantage that the method usually has no difficulty in finding corresponding points. Therefore, measurement is more reliable than structure from motion analysis and the method is used in various fields [11][12].

However, in general, the light section method requires that the position and the orientation of the camera be constant while measurement. If the camera moves, it is difficult to integrate of the measurement results. Therefore, the camera motion estimation (the relative relations of camera positions and orientations) is important for the measurement. The idea of light section method with omni-directional camera can be found in works such as papers [13][14].

Yi et al. do not describe camera motion estimation. Orghidan et al. proposed a camera motion estimation method based on ICP algorithm. However, the method is difficult for estimation of six degrees of freedom. On the other hand, the structure from motion analysis has the advantage that it can estimate the camera motion with 3-D measurement. Thus, the method is used not only for pipe inspection but also for construction of an environment map [15][16].

We have already proposed a reconstruction method of pipe shape with a light section method and a structure from motion analysis [17]. There is a problem that the texture information was not considered. The texture information is important for pipe inspection. Therefore, a 3-D pipe model which has shape information and texture information is effective for recognition of pipe state.

In this paper, we propose a 3-D measurement method using an omni-directional camera and an omni-directional laser with a light section method and a structure from motion analysis. Our method calculates 3-D coordinates by the light section method. The individual measurement data is integrated with

K. Matsui, A. Yamashita and T. Kaneko are with Department of Mechanical Engineering, Shizuoka University, 3–5–1 Johoku, Naka-ku, Hamamatsu-shi, Shizuoka 432–8561, Japan (phone: 053-478-1604; fax: 053-478-1604; e-mail: {f0930058, tayamas, tmtkane}@ipc.shizuoka.ac.jp)

the information of camera motion estimated by the structure from motion analysis. By pasting textures on the measurement data, a 3D Pipe model is generated.

II. OUTLINE

An inspection robot executes 3-D measurement by using a rangefinder constructed with a omni-directional camera (Fig.1) and a laser source that can emit laser light in all direction orthogonal to the head (Fig.2).

The process of our method is shown in Fig.3. As the first step, the inspection robot acquires an omni-directional image sequence during its locomotion while emitting laser light.

The second step calculates 3-D coordinates of measurement points by the light section method.

The third step estimates a camera motion by the structure from motion method and integrates measurement results.

Finally, a triangular mesh is generated from the measurement results. By texture mapping to the triangular mesh, the 3-D model of pipe is reconstructed.

Fig.1 Omni-directional camera

Fig.2 Omni-directional laser

III. 3-D MEASUREMNT

We use the light section method for 3-D measurement.

First, we extract image coordinates of laser light from an omni-directional image sequence.

Then, the 3-D coordinates of measurement point are given as the cross-point of a ray vector and the laser light.

A. Laser Light Extraction

The laser light reflected by the measurement object is captured by the omni-directional camera as a circular area with some width. Therefore, we have to extract the peak (the pixel that has the highest intensity) from the area that can be considered as the laser light on image. We use the Gaussian approximation method [18] to extract the peak.

In order to detect the laser light, we scan radially around the center of the omni-directional image (Fig.4). We approximate the changing of intensity value in the radial direction to the Gaussian distribution (Fig.5).

Then, we select the three highest intensity values from the laser light. The subpixel offset d is calculated from these values by Eq.(1).

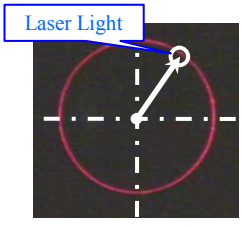

Fig.4 Radial scanning

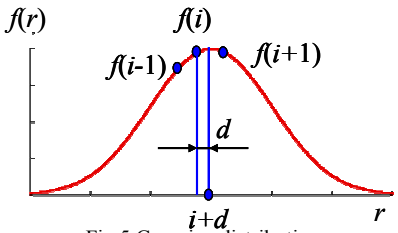

Fig.5 Gaussian distribution

$$d = \frac{1}{2}\frac{\ln(f(i-1)) - \ln(f(i+1))}{\ln(f(i-1)) - 2\ln(f(i)) + \ln(f(i+1))} \quad (1)$$

where $f(i)$ denotes the intensity at i which is an image coordinate of the observed peak.As a result, $(i + d)$ is obtained as the image coordinate of the laser light.

B. 3-D Coordinates Calculation

We define a unit vector which starts at the center of projection and ends at a measurement point in 3D space as a ray vector $\mathbf{r} = [x, y, z]^T$, where T stands for transposition of a vector.

The omni-directional camera has a hyperboloid mirror in front of lens of a conventional camera. Therefore, as shown in Fig.6, ray vector $\mathbf{r}$ is directed from the focus of the hyperboloid mirror to the reflection point of the ray on the mirror surface.

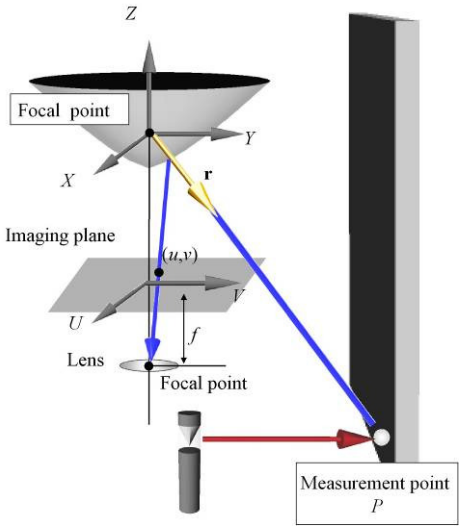

Fig.6 Calculation of 3-D coordinates

Ray vector $\mathbf{r}$ is calculated from image coordinates $[u, v]$ of the laser light using Eqs.(2), (3) and (4). In these equations, a, b and c are the hyperboloid parameters, and f is the image distance (the distance between the center of the lens and the image plane) of camera. λ represents the scale of a ray vector.

$$\mathbf{r} = \lambda \begin{bmatrix} su \\ sv \\ sf - 2c \end{bmatrix} \quad (2)$$

$$s = \frac{a^2(f\sqrt{a^2+b^2} + b\sqrt{u^2+v^2+f^2})}{a^2f^2 - b^2(u^2+v^2)} \quad (3)$$

$$c = \sqrt{a^2+b^2} \quad (4)$$

Then, we define the plane of laser light as Eq.(5). In the equation, k_1, k_2, k_3, k_4 are the planar parameters, and which calibrated in advance.

$$k_1x + k_2y + k_3z + k_4 = 0 \quad (5)$$

From Eqs.(2), (3), (4) and (5) the 3-D coordinates of the

measurement point is calculated by Eq.(6).

$$\begin{bmatrix} x_p \\ y_p \\ z_p \end{bmatrix} = \frac{-k_4}{k_1 su + k_2 sv + k_3 (sf - 2c)} \begin{bmatrix} su \\ sv \\ sf - 2c \end{bmatrix} \quad (6)$$

IV. CAMERA MOTION ESTIMATION

We use a structure from motion analysis for camera motion estimation [19].

First, the robot acquires an omni-directional image sequence during its locomotion.

Second, the method extracts and tracks feature points to get corresponding points in the omni-directional image sequence.

The camera motion is estimated by the linear estimation, which uses the positions of corresponding points in two images taken at each observation point.

In order to estimate the camera motion more precisely, re-estimation of camera motion is performed with nonlinear estimation.

A. Corresponding Point Acquisition

For getting corresponding points between images in the omni-directional image sequence, the method extracts feature points in the first image and then tracks them along the sequence. In our method, we use SIFT (Scale Invariant Feature Transform) algorithm [20].

First, we extract feature points. By comparing these points between two images taken before and after the robot movement, we get corresponding points which are regarded as the same point in 3-D space (Fig.7).

B. Estimation of Camera Motion

In order to estimate camera motion, we calculate the essential matrix which contains information about relative position and orientation differences between two observation points.

Essential Matrix **E** satisfies Eq.(7).

$$\mathbf{r}_i'^T \mathbf{E} \mathbf{r}_i = 0 \quad (7)$$

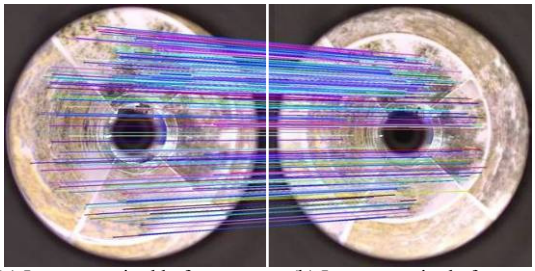

(a) Image acquired before robot movement (b) Image acquired after robot movement

Fig.7 Corresponding point acquisition

where $\mathbf{r}_i = [x_i, y_i, z_i]^T$, $\mathbf{r}_i' = [x'_i, y'_i, z'_i]^T$ are the ray vectors of the corresponding point in two images, respectively. Equation (7) is transformed into Eq.(8).

$$\mathbf{u}_i^T \mathbf{e} = 0 \quad (8)$$

where

$\mathbf{u}_i = [x_i x'_i, y_i x'_i, z_i x'_i, x_i y'_i, y_i y'_i, z_i y'_i, x_i z'_i, y_i z'_i, z_i z'_i]^T$

$\mathbf{e} = [e_{11}, e_{12}, e_{13}, e_{21}, e_{22}, e_{23}, e_{31}, e_{32}, e_{33}]^T$

Essential matrix **E** is obtained by solving simultaneous equations for more than eight pairs of corresponding ray vectors. This means that we solve Eq.(9).

$$\min_e \|\mathbf{U}\mathbf{e}\|^2 \quad (9)$$

where $\mathbf{U} = [\mathbf{u}_1, \mathbf{u}_2, \cdots, \mathbf{u}_n]^T$. Essential matrix **E** is obtained from **e** which is given as the eigenvector of the smallest eigenvalue of $\mathbf{U}^T\mathbf{U}$.

From essential matrix **E**, we calculate rotation matrix **R** and translation vector **t**.

Essential matrix **E** is represented by rotation matrix **R** and translation vector $\mathbf{t} = [t_x, t_y, t_z]^T$.

$$\mathbf{E} = \mathbf{RT} \quad (10)$$

Here, **T** is a matrix given as follows.

$$\mathbf{T} = \begin{bmatrix} 0 & -t_z & t_y \\ t_z & 0 & -t_x \\ -t_y & t_x & 0 \end{bmatrix} \quad (11)$$

However, all feature points tracked along the image sequence do not behave as corresponding points because of image noise. Mistracked Feature points should be rejected as outliers. To solve this problem, we employ a method of RANSAC (RANdom SAmple Consensus) [21].

In the procedure, we select randomly eight feature points, which are the minimum number of points for determining essential matrix **E**. Let $\mathbf{E}_{\text{rand}}$ be the essential matrix determined by using these feature points, and k be the number of feature points satisfying Eq.(12), where q is a given threshold.

$$\left| \mathbf{r}_i'^T \mathbf{E}_{\text{rand}} \mathbf{r}_i \right| < q \quad (12)$$

We repeat this process of determining essential matrix $\mathbf{E}_{\text{rand}}$ and number k for predetermined times. Then we choose the case with the maximum number of k, and remove feature points that do not satisfy Eq.(12) as outliers.

Finally, we calculate essential matrix **E** by Eq.(9) using the remaining feature points.

C. Re-Estimation of Camera Motion

The Rotation matrix and the translation vector estimated in Section 4.3 may not be always good results because of various errors in images. Then, we re-estimate the camera motion in consideration of the measurement errors in each feature point.

We use bundle adjustment [22] for re-estimation of the camera motion. The method minimizes the sum of feature reprojection errors which means difference between the image coordinates of the original feature point and the reprojected point.

D. Scale Match Method

The structure from motion analysis cannot determine the distance $|\mathbf{t}|$ between two observation points because the measurement only uses images for input and does not get any scale information.

However, the 3-D coordinates of point measured by the light section method includes scale information. Therefore, we use the measurement result by the light section method for scale matching.

First, we measure the 3-D coordinates of a point by the light section method. The 3-D coordinates of the same point are measured by the structure from motion analysis (the green circle in Fig.8). The ray vector is calculated from corresponding points. Template matching based on normalized cross-correlation is used for getting corresponding points. Then, the 3-D coordinates of the point are given as those of the cross-point of two ray vectors.

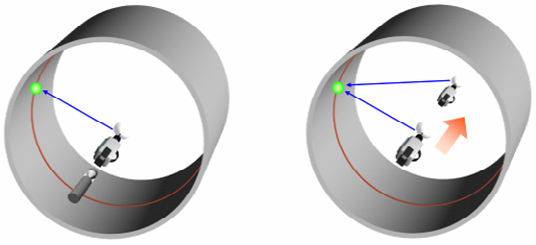

(a) Measurement by light section method

(b) Measurement by structure from motion

Fig.8 Scale matching

Scale matching is realized by making the 3-D coordinates of the same point as close as possible. Minimization of deviation of the two resultant coordinates of the same point is more sensitive when the point lies farther from the observation point. Therefore it is appropriate to minimize the distances of coordinates. Scale s' is calculated by Eq.(13).

$$\min \sum_{k=1}^{m} \left\| \log(\mathbf{p}_k) - \log(s'\mathbf{p}_k) \right\|^2 \qquad (13)$$

where $\mathbf{p}_k = [x_k,\ y_k,\ z_k]^T$ represents the measurement result by the light section method, and $\mathbf{p}_k' = [x_k', y_k', z_k']^T$ represents the measurement result by the structure from motion analysis. By the procedure, we can integrate the individual measurement data with matched scale.

V. TEXTURE MAPPING

A triangular mesh is generated from integrated measurement data by using the 3-D Delaunay triangulation. But, the Delaunay triangulation generates a triangular mesh which contradicts a physical shape because the triangular mesh does not consider the shape of the measurement object. Therefore, we apply the triangular optimization method [23] to the triangular mesh. The method adapts the triangular mesh to the physical shape by detecting a texture distortion. By texture mapping to the triangular mesh, a 3-D environment model is constructed.

VI. EXPERIMENTS

In the experiment we measured two objects. One is a rectangular container and the other is a pipe. The size of input image is 1920x1080 pixels.

In 3-D measurement, we used images without ambient illumination. Also, in camera motion estimation, we used images with ambient illumination.

A. Accuracy Evaluation Experiment

The experimental environment is shown in Fig.9.

We fixed an omni-directional camera and an omni-directional laser to a jig (Fig.10). The laser light was emitting while lifting the jig in container. Then, we acquired an image sequence by using the omni-directional camera.

Figures 11 and 12 show acquired images with ambient illumination and without ambient illumination. Figure 13 shows the result of measurement. The result shows our proposed method can reconstruct the 3-D shape of the container.

Table 1 shows the standard deviations from the least square planes. Table 2 shows angles between two planes calculated by a least square method and Table 3 shows the distances between corner points.

The errors of distances between corner points are within the theoretical value of our proposed method.

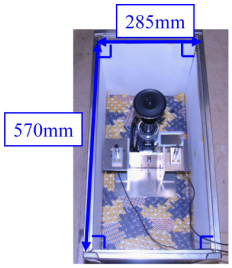

Fig.9 Experimental environment 1

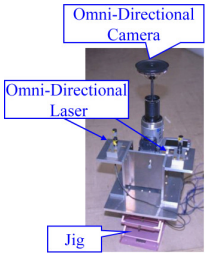

Fig.10 Measurement device 1

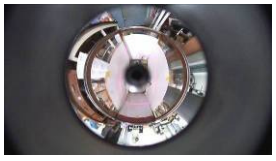

Fig.11 Image with ambient illumination 1

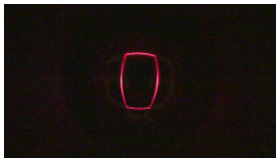

Fig.12 Image without ambient illumination 1

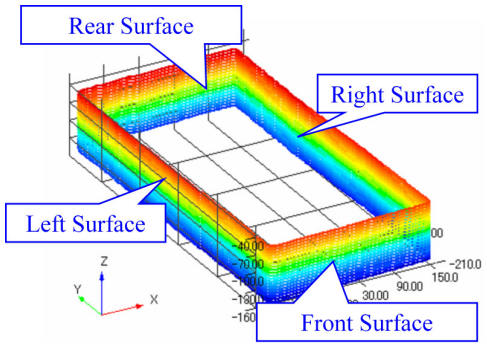

Fig.13 Reconstruct of container

Table 1 Standard deviations from the least square error plane

	Standard deviation
Front Surface	1.08mm
Rear Surface	0.88mm
Left Surface	0.85mm
Right Surface	0.69mm

Table 2 Angles between two least square error planes

	Measurement value	Ground truth
Front and Left Surfaces	90.4deg	90.0deg
Rear Surface and Left Surface	89.6deg	90.0deg
Front Surface and Right Surface	90.6deg	90.0deg
Rear Surface and Right Surface	89.4deg	90.0deg

Table 3 Distances between corner points

	Measurement value	Ground truth
Front Surface	282mm	285mm
Rear Surface	283mm	285mm
Left Surface	567mm	570mm
Right Surface	568mm	570mm

B. *Measurement Experiment*

We prepare a pipe as a measurement object and performed an accuracy evaluation of shape reconstruction. Also we prepare a manipulator and installed an omni-directional camera and an omni-directional laser. The accuracy evaluation of camera motion estimation is performed by using the trajectory information of manipulator

The experimental environment is shown in Fig.14. Figure 15 shows the actual image of the pipe. Assuming the case where the imperfection exists in the pipe, we added a projection to the pipe as shown in Fig. 16. The camera moved with the manipulator as shown in Fig. 17.The laser light was emitting while the manipulator moved in the pipe. Then, we acquired an image sequence by using the omni-directional camera.

Figures 18 and 19 show acquired images with ambient illumination and without ambient illumination, respectively.

Figure 20 shows the estimated camera motion. Color points represent the measurement results. Black points represent the ground truth. Table 4 shows the accuracy evaluations of estimated camera motion. Our proposed method can estimate the camera motion within a 3mm error margin.

These results show our proposed method can estimate camera motion while the camera moves arbitrarily.

Figures 21 and 22 show the result with our proposed method and the result using movement information of the manipulator. (a) is the bird's eye view of the experimental result. (b) is the top view of the experimental result.

By comparing Figs.21 to 22, we can say our proposed method can reconstruct the pipe shape with high precision.

Table 5 shows comparison of the ground truth values and the measurement data. In Table 5, the measurement value of the inside diameter is calculated by cylinder fitting. The result shows our proposed method can measure the pipe with high precision.

Figures 23 and 24 shows the experimental result of texture mapping. (a) is the front view. (b) is the internal view. The result shows our proposed method can measure the pipe in detail. By using texture information, recognition of the convex part becomes easy.

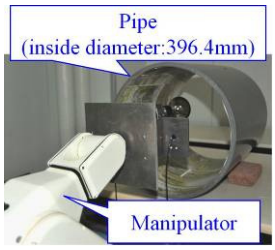

Fig.14 Experimental environment 2

Fig.15 Actual image

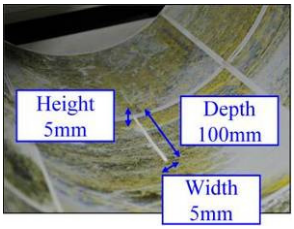

Fig. 16 Projection

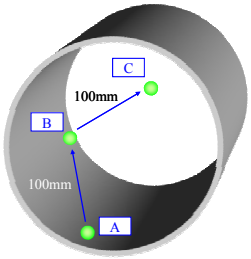

Fig.17 Experimental trajectory of the manipulator

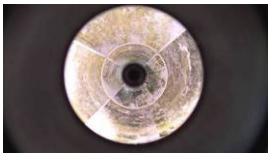

Fig.18 Image with ambient illumination 2

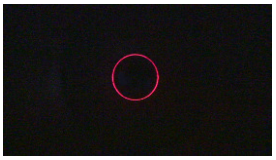

Fig.19 Image without ambient illumination 2

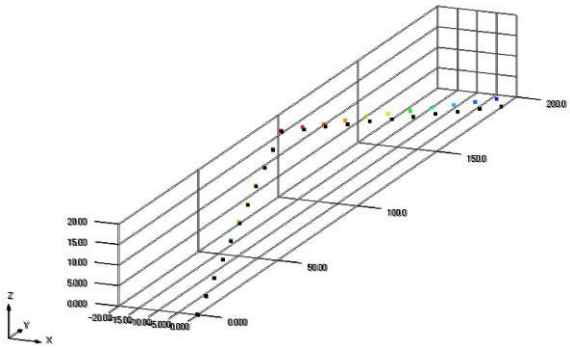

Fig.20 Estimated camera motion

Table 4 Accuracy evaluations of estimated camera motion

	Measurement value	Ground truth
Between A and B	102mm	100mm
Between B and C	103mm	100mm

VII. CONCLUSIONS

In this paper, we propose a reconstruction method of pipe shape by using an omni-directional laser and an omni-directional camera with a light section method and a structure from motion analysis. Experimental results showed the effectiveness of the proposed method.

As future works, we should improve the proposed rangefinder to emit an illumination light. Also we should install the proposed rangefinder to inspection robot.

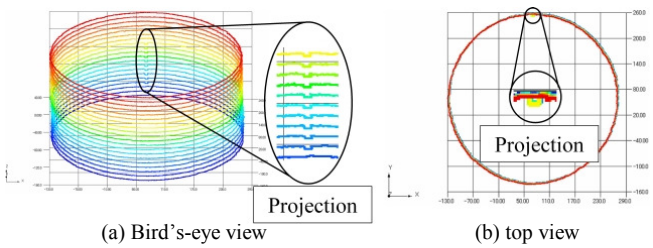

(a) Bird's-eye view (b) top view

Fig.21 Reconstruction of pipe shape with the proposed method

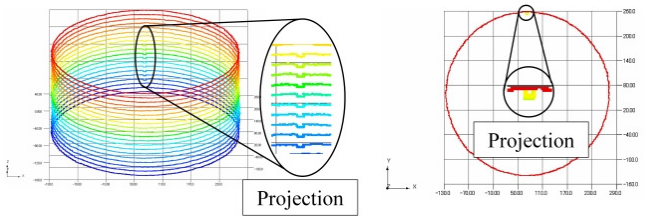

(a) Bird's-eye view (b) top view

Fig.22 Reconstruction of pipe shape with movement information of manipulator

Table 5 Accuracy evaluation

	Measurement value	Ground truth
Inside diameter	394.8mm	396.4mm
Height	8mm	5mm
Width	7mm	5mm
Depth	103mm	100mm

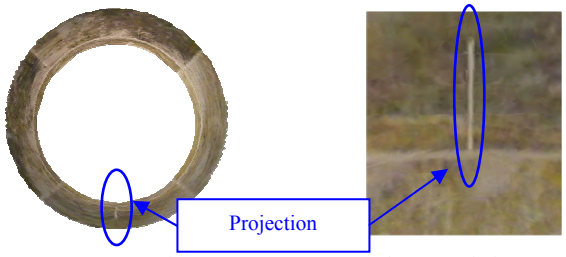

(a) Front view (b) Internal view

Fig.23 Result of texture mapping with our proposed method

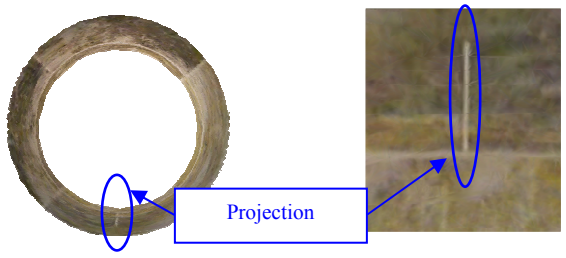

(a) Front view (b) Internal view

Fig.24 Result of texture mapping with movement information of manipulator

References

[1] A. Ahrary, A..A.F Nassiraei and M. Ishikawa, "A Study of An autonomous Mobile Robot for a Sewer Inspection System," Journal of Artificial Life and Robotics, Vol.11, No.1, pp.23-27, 2007.

[2] K.U. Scholl, V. Kepplin, K. Berns, and R. Dillmann, "Controlling a Multijoint Robot for Autonomous Sewer Inspection," Proceedings of the 2000 IEEE International Conference on Robotics and Automation (ICRA 2000), pp.1701-1706, 2000.

[3] H.B. Kuntze and H. Haffner, "Experiences with the Development of a Robot for Smart Multisensoric Pipe Inspection," Proceedings of the 1998 IEEE International Conference on Robotics and Automation (ICRA 1998), pp.1773-1778, 1998.

[4] A. Zagler, and F. Pfeiffer, "MORITZ a Pipe Crawler for Tube Junctions," Proceedings of the 2003 IEEE International Conference on Robotics and Automation (ICRA 2003), pp.2954-2959, 2003.

[5] M.Horodinca, I.Doroftei and E.Mignon, "A Simple Architecture for In-Pipe Inspection Robots," Proceedings of the 2002 International Colloquium on Mobile and Autonomous Systems, (ICMAS 2002), pp.1-4, 2002.

[6] K. Suzumori, S. Wakimoto and M. Tanaka, "A Miniature Inspection Robot Negotiating Pipes of Widely Varying Diameter," Proceedings of the 2003 IEEE International Conference on Robotics and Automation (ICRA 2003), pp.2735-2740, 2003.

[7] J. Gaspar, N. Winters and J. S. Victor, "Vision-Based Navigation and Environmental Representations with an Omnidirectional Camera," IEEE Transactions on Robotics and Automation, Vol.16, No.6, pp.890-898, 2000.

[8] Y. Yagi, "Omnidirectional Sensing and Its Applications," IEICE Transactions on Information and Systems, Vol.E82-D, No.3, pp.568-579, 1999.

[9] J. Gluckman, and S. K. Nayar, "Ego-motion and Omnidirectional Cameras," Proceedings of the 6th International Conference on Computer Vision, pp.999-1005, 1998.

[10] J. Kannala, S. S. Brandt, and J. Heikkilä, "Measuring and Modelling Sewer Pipes from Video," Machine Vision and Applications, Vol.19, No.2, pp.73-83, 2008.

[11] A. Yamashita, H. Higuchi and T. Kaneko, "Three Dimensional Measurement of Object's Surface in Water Using the Light Stripe Projection Method," Proceedings of the 2004 IEEE International Conference on Robotics and Automation (ICRA2004), pp.2736-2741, 2004.

[12] Y. Yachide, Y. Oike, M. Ikeda. and K. Asada, "Real-time 3-D Measurement System Based on Lght-Section Method Using Smart Image Sensor," Proceedings of the 2005 IEEE International Conference on Image Processing (ICIP 2005), pp.III-1008-1011, 2005.

[13] S. Yi, B. Choi, and N. Ahuja: "Real-time Omni-directional Distance Measurement with Active Panoramic Vision", International Journal of Control, Automation, and Systems, Vol.5, No.2, pp.184–191, 2007.

[14] R. Orghidan, E. Mouaddib, J. Salvi: "Omni-directional Depth Computation from a Single Image", Proceedings of the 2005 IEEE International Conference on Robotics and Automation, pp.1234–1239, 2005.

[15] B. Micusik and T. Pajdla: "Structure from Motion with Wide Circular Field of View Cameras", IEEE Transactions on Pattern Analysis and Machine Intelligence, Vol.28, No.7, pp.1135–1149, 2006.

[16] M. Lhuillier: "Automatic Scene Structure and Camera Motion using a Catadioptric System", Computer Vision and Image Understanding, Vol.109, No.2, pp.186–203, 2008.

[17] K. Matsui, A. Yamashita and T. Kaneko, "3-D Shape Reconstruction of Pipe with Omni-Directional Laser and Omni-Directional Camera," Proceedings of the 3rd International Conference of Asian Society for Precision Engineering and Nanotechnology (ASPEN2009), 1A2-15, pp.1-5, 2009.

[18] R.B.Fisher and D.K.Naidu, "A Comparison of Algorithms for Subpixel Peak Detection," Proceedings of the 1991 British Machine Vision Association Conference (BMVAC 1991), pp.217-225, 1991.

[19] R. Kawanishi, A. Yamashita and T. Kaneko, "Estimation of Camera Motion with Feature Flow Model for 3D Environment Modeling by Using Omni-Directional Camera," Proceedings of the 2009 IEEE/RSJ International Conference on Intelligent Robots and Systems (IROS2009), 2009.

[20] D. G. Lowe, "Distinctive Image Features from Scale-Invariant Keypoints," International Journal of Computer Vision, Vol.60, No.2, pp.91-110, 2004.

[21] M. A. Fischler and R. C. Bolles, "Random Sample Consensus: A Paradigm for Model Fitting with Applications to Image Analysis and Automated Cartography," Communications of the ACM, Vol.24, No.6, pp.381-395, 1981.

[22] B. Triggs, P. McLauchlan, R. Hartley and A. Fitzgibbon, "Bundle Adjustment -A Modern Synthesis," Vision Algorithms: Theory & Practice, Springer-Verlag LNCS 1883, 2000.

[23] A. Nakatsuji, Y. Sugaya, and K. Kanatani, "Optimizing a Triangular Mesh for Shape Reconstruction from Images," IEICE Transactions on Information and Systems, Vol. E88-D, No. 10, pp. 2269-2276, 2005.